Stable and Unstable Phases of a Diblock Copolymer Melt

M. W. Matsen and M. Schick
Department of Physics FM-15, University of Washington, Seattle, Washington 98195
(Received 15 December 1993; revised manuscript received 25 February 1994)

Using self-consistent field theory, we examine microphases of diblock copolymers and find, in addition to lamellar, hexagonal, and cubic phases, a stable gyroid phase which occurs between the lamellar and hexagonal ones. It terminates at a triple point, with a lamellar to hexagonal transition occurring in the weak-segregation limit. Other phases of experimental interest are studied, and we describe the regions in which they are most nearly stable.

PACS numbers: 83.70.Hq, 36.20.−r, 61.25.Hq, 64.60.Cn

Diblock copolymer melts have received much attention over the past few years due in large part to their ability to assemble into various ordered structures. They do so in order to reduce the number of energetically unfavorable contacts between the two different blocks comprising the polymer molecule. The simplest of these ordered microphases is the lamellar (L) phase in which the A and B monomers separate into A-rich and B-rich lamellae. It is observed to occur when the volume fractions of the two monomers are comparable. If the volume fraction of one monomer becomes sufficiently greater than that of the other, the minority component is observed to form cylinders which pack in a hexagonal arrangement, forming the hexagonal (H) phase. With increasing asymmetry in the volume fractions, the minority component forms spheres which then pack in a body-centered cubic arrangement, the cubic (C) phase. At first, these were the only ordered phases to be observed. Later, several new phases were detected between the L and H phases. Given the difficulty of achieving equilibrium in these systems, it was not clear whether all of the new phases observed were thermodynamically stable. The most frequently observed of them is the ordered, bicontinuous, double-diamond (OBDD) phase [1–3]. In it, the minority component forms two separate interpenetrating diamond lattices. Catenoid-lamellar (CL) phases have also been observed [1,2,4–7]. These are lamellar phases in which the lamellae of the majority component are joined by tubes which perforate the minority lamellae. If the lamellae of the minority component are similarly joined, then the phase is bicontinuous [1]; if not, it is monocontinuous. The tubes perforating the lamellae form a triangular array, with the array of tubes in one minority lamellae staggered with respect to those in the next [4,5]. It has not been determined whether the stacking of these tubes is of the form *abab*... or *abcabc*.... We shall label the phases with these stackings as CL_{ab} and CL_{abc}, respectively, and the analogous phase in which the tubes are aligned from one lamellae to the next as CL_{a} [8,9]. Most recently, a gyroid (G) phase has been observed [10]. This is a bicontinuous phase in which the minority component forms two separate interpenetrating lattices which are threefold coordinated, and mirror images of one another. Either lattice, by itself, belongs to the space group $I4_132$; the full structure comprising both lattices belongs to the space group $Ia3d$ [11].

The theory of copolymer phases is well understood; it is simply the mean, or self-consistent, field theory (SCFT) adapted to polymers [12,13]. Like all mean-field theories, it ignores the effect of thermal fluctuations. While this effect is observable in the ordering transitions from the disordered phase, the temperature region in which these fluctuations are important scales as an inverse power of the polymerization index and hence is small for most systems studied [14]. Thus the SCFT should predict the phase diagram well over almost the whole temperature region. At first this seemed to be the case, because the theory does predict the L, H, and C phases [15,16]. However, the theory has never predicted either the stability or near stability of *any* of the more recently observed phases, which has cast some doubt on its applicability or, at least, its utility.

In this Letter, we show that such doubts are unfounded by illustrating that the self-consistent equations can be solved to examine the stability of all of the phases which have been reported, and others closely related to them. We find in addition to the L, H, and C microphases that the G phase is also stable and occurs between L and H phases. This phase terminates at a triple point. An L to H transition occurs for weak segregation, and along it bicontinuous CL phases are close to stability. For intermediate segregation, the free energy of the stable G phase is only slightly lower than that of the monocontinuous CL_{ab} and CL_{abc} phases, and their free energies are, in turn, only slightly lower than that of the OBDD phase. We cannot perform our calculations in the strong-segregation limit.

We consider a system of n AB diblock copolymers each of polymerization, N, and A-monomer fraction, f. We assume that the A and B monomers occupy a fixed volume, $1/\rho_0$, and that the system is incompressible with a total volume, V, equal to nN/ρ_0. Each polymer is parametrized with a variable s that increases continuously along its length. At the A-monomer end, $s = 0$, at the junction point, $s = f$, and at the other end, $s = 1$. Using this parametrization, we define functions, $\mathbf{r}_\alpha(s)$,

0031-9007/94/72(16)/2660(4)$06.00

that specify the space curve occupied by the αth copolymer.

The partition function we use for this system is

$$Z = \int \prod_{\alpha=1}^{n} \tilde{\mathcal{D}}\mathbf{r}_\alpha \, \delta[1 - \hat{\phi}_A - \hat{\phi}_B] \exp\left\{ -\chi\rho_0 \int d\mathbf{r} \, \hat{\phi}_A \hat{\phi}_B \right\} ,$$

where the functional integral over all configurations is weighted, $\tilde{\mathcal{D}}\mathbf{r}_\alpha \equiv \mathcal{D}\mathbf{r}_\alpha \, P[\mathbf{r}_\alpha; 0, 1]$, with the functionals

$$P[\mathbf{r}_\alpha; s_1, s_2] \propto \exp\left\{ -\frac{3}{2Na^2} \int_{s_1}^{s_2} ds \left| \frac{d}{ds} \mathbf{r}_\alpha(s) \right|^2 \right\} .$$

The Kuhn length, a, is assumed to be the same for both monomers. The delta functional selects out only those configurations satisfying the incompressibility constraint. The Flory-Huggins parameter, χ, measures the incompatibility between A and B monomers. The dimensionless A monomer-density operator is given by

$$\hat{\phi}_A(\mathbf{r}) = \frac{N}{\rho_0} \sum_{\alpha=1}^{n} \int_0^f ds \; \delta(\mathbf{r} - \mathbf{r}_\alpha(s)) ,$$

and $\hat{\phi}_B$ by a similar expression. To make the expression for Z more tractable [12], one inserts a functional integral, $1 = \int \mathcal{D}\Phi_A \, \delta[\Phi_A - \hat{\phi}_A]$, which permits the replacement of the operator $\hat{\phi}_A$ by the function Φ_A. Doing the same for $\hat{\phi}_B$ and inserting standard integral representations for the delta functionals, one obtains

$$Z = \mathcal{N} \int \mathcal{D}\Phi_A \, \mathcal{D}W_A \mathcal{D}\Phi_B \, \mathcal{D}W_B \, \mathcal{D}\Xi \exp\{-F/k_BT\} , \tag{1}$$

where $\mathcal{N}$ is a normalization constant,

$$F/nk_BT \equiv -\ln \mathcal{Q} + V^{-1} \int d\mathbf{r} [\chi N \Phi_A \Phi_B - W_A \Phi_A - W_B \Phi_B - \Xi(1 - \Phi_A - \Phi_B)] , \tag{2}$$

$$\mathcal{Q} \equiv \int \tilde{\mathcal{D}}\mathbf{r}_\alpha \exp\left\{ -\int_0^f ds \, W_A(\mathbf{r}_\alpha) - \int_f^1 ds \, W_B(\mathbf{r}_\alpha) \right\} .$$

The functional $F[\Phi_A, W_A, \Phi_B, W_B, \Xi]$ can be evaluated exactly, but the functional integrals in Eq. (1) cannot. In the SCFT [12], one approximates this integral by the extremum of the integrand. Thus the free energy, $-k_BT \ln Z$, is given by $F[\phi_A, w_A, \phi_B, w_B, \xi]$, where ϕ_A, w_A, ϕ_B, w_B, and ξ are the functions for which F attains its minimum. From its definition, Eq. (2), it follows that these functions satisfy the self-consistent equations

$$w_A(\mathbf{r}) = \chi N \phi_B(\mathbf{r}) + \xi(\mathbf{r}) , \tag{3}$$

$$w_B(\mathbf{r}) = \chi N \phi_A(\mathbf{r}) + \xi(\mathbf{r}) , \tag{4}$$

$$\phi_A(\mathbf{r}) + \phi_B(\mathbf{r}) = 1 , \tag{5}$$

$$\phi_A = -\frac{V}{\mathcal{Q}} \frac{\mathcal{D}\mathcal{Q}}{\mathcal{D}w_A} , \tag{6}$$

$$\phi_B = -\frac{V}{\mathcal{Q}} \frac{\mathcal{D}\mathcal{Q}}{\mathcal{D}w_B} . \tag{7}$$

The last two equations identify $\phi_A(\mathbf{r})$ and $\phi_B(\mathbf{r})$ as the average densities of A and B monomers at $\mathbf{r}$ as calculated in an ensemble of noninteracting polymers subject to the fields, $w_A(\mathbf{r})$ and $w_B(\mathbf{r})$, which act on A and B monomers, respectively. The SCFT approximation has reduced the problem to one of a single noninteracting polymer in external fields. Once the partition function of this problem, $\mathcal{Q}[w_A, w_B]$, is known, Eqs. (3)–(6) can be solved and the free energy obtained.

It is at this point that additional approximations are often made, such as expanding $\ln \mathcal{Q}$ in cumulants, and keeping only the first few terms [8,15]. Such additional approximations may be convenient at times, but are unnecessary because the exact expression for $\mathcal{Q}$ can be evaluated. One writes the partition function as $\mathcal{Q} = \int d\mathbf{r} \; q(\mathbf{r}, 1)$, where

$$q(\mathbf{r}, s) = \int \mathcal{D}\mathbf{r}_\alpha \, P[\mathbf{r}_\alpha; 0, s] \delta(\mathbf{r} - \mathbf{r}_\alpha(s)) \exp\left\{ -\int_0^s dt \times [\gamma(t) w_A(\mathbf{r}_\alpha(t)) + (1 - \gamma(t)) w_B(\mathbf{r}_\alpha(t))] \right\} \tag{8}$$

is the end-segment distribution function. The step function, $\gamma(s)$, is 1 for $s < f$ and 0 otherwise. This distribution function satisfies the modified diffusion equation,

$$\frac{\partial q}{\partial s} \equiv \begin{cases} \frac{1}{6} Na^2 \nabla^2 q - w_A(\mathbf{r}) q, & \text{if } s < f , \\ \frac{1}{6} Na^2 \nabla^2 q - w_B(\mathbf{r}) q, & \text{if } s > f , \end{cases} \tag{9}$$

and the initial condition, $q(\mathbf{r}, 0) = 1$ [13]. Because the two ends of the copolymer are distinct, a second end-segment distribution function, $q^\dagger(\mathbf{r}, s)$, is defined with an almost identical definition, Eq. (8), except that the functional integration over $\mathbf{r}_\alpha(t)$ is done for $t = s$ to 1. It satisfies $q^\dagger(\mathbf{r}, 1) = 1$, and Eq. (9) with the right-hand side multiplied by -1. In terms of these functions, the A-monomer density, Eq. (5), is

$$\phi_A(\mathbf{r}) = \frac{V}{\mathcal{Q}} \int_0^f ds \; q(\mathbf{r}, s) \, q^\dagger(\mathbf{r}, s) . \tag{10}$$

The expression for $\phi_B(\mathbf{r})$ is similar.

Rather than attempting to solve the above problem in real space, we expand functions of position, $g(\mathbf{r})$, as $\sum_i g_i f_i(\mathbf{r})$, where $f_i(\mathbf{r})$, $i = 1,2,3,...$, are orthonormal basis functions [i.e., $V^{-1} \int f_i(\mathbf{r}) f_j(\mathbf{r}) d\mathbf{r} = \delta_{ij}$] each possessing the symmetry of the phase being considered. They are chosen to be eigenfunctions of the Laplacian operator; $\nabla^2 f_i(\mathbf{r}) = -\lambda_i D^{-2} f_i(\mathbf{r})$, where D is a length scale for the phase [17]. We order the functions starting with $f_1(\mathbf{r}) = 1$ such that λ_i is a nondecreasing series. In this basis, the diffusion equation (9) for $q(\mathbf{r}, s)$ becomes

$$\frac{dq_i(s)}{ds} = \begin{cases} \sum_j A_{ij} q_j(s), & \text{if } s < f \ , \\ \sum_j B_{ij} q_j(s), & \text{if } s > f \ , \end{cases}$$

$$A_{ij} = -\tfrac{1}{6} N a^2 \lambda_i D^{-2} \delta_{ij} - \sum_k w_{A,k} \Gamma_{ijk} \ , \qquad (11)$$

where $\Gamma_{ijk} = V^{-1} \int f_i(\mathbf{r}) f_j(\mathbf{r}) f_k(\mathbf{r}) d\mathbf{r}$ and the matrix, B, is given by a similar expression to Eq. (11). The initial condition is $q_i(0) = \delta_{i1}$. The solution to this set of linear differential equations is

$$q_i(s) = \begin{cases} T_{A,i1}(s), & \text{if } s < f \ , \\ \sum_j T_{B,ij}(s-f)\, T_{A,j1}(f), & \text{if } s > f \ , \end{cases}$$

where $T_A(s') \equiv \exp(As')$ and $T_B(s') \equiv \exp(Bs')$ are matrices that transfer $q_i(s)$ a distance s' along A and B regions of the copolymer, respectively. These matrices are easily evaluated by performing an orthogonal transformation that diagonalizes either A or B. Similarly,

$$q_i^\dagger(s) = \begin{cases} \sum_j T_{A,ij}(f-s)\, T_{B,j1}(1-f), & \text{if } s < f \ , \\ T_{B,i1}(1-s), & \text{if } s > f \ . \end{cases}$$

Now that the amplitudes of the end-segment distribution functions are known, $\mathcal{Q}$ is given by $Vq_1(1)$, the amplitudes of $\phi_A(\mathbf{r})$, Eq. (5), are

$$\phi_{A,i} = \frac{1}{q_1(1)} \int_0^f ds \sum_{jk} q_j(s)\, q_k^\dagger(s)\, \Gamma_{ijk} \ ,$$

and the amplitudes $\phi_{B,i}$ are given by a similar expression. We adjust the amplitudes $w_{A,i}$ and $w_{B,i}$ of the fields so that the densities calculated from them satisfy $\phi_{B,i} = -\phi_{A,i} = (w_{A,i} - w_{B,i})/2\chi N$, Eqs. (3)–(4). For $i = 1$, we may set $\xi_1 = 0$, so that $\omega_{A,1} = \chi N \phi_{B,1}$ and $\omega_{B,1} = \chi N \phi_{A,1}$. This completes the cycle of self-consistent equations. The free energy, Eq. (2), to within an additive constant can be written

$$F/nk_BT = -\ln[q_1(1)] - \chi N \sum_i \phi_{A,i}\, \phi_{B,i} \ .$$

For the disordered phase, $F/nk_BT = \chi N f(1-f)$. When dealing with an ordered periodic phase, we minimize this free energy with respect to its wavelength, D. For CL phases, there are two wavelengths. By comparing the free energies for different phases, we obtain the phase diagram shown in Fig. 1.

The notable aspect of this diagram is that, in addition to the usual L, H, and C phases [16], there exist G phases. Unlike the other phases which all extend to the critical point, the G phases end at triple points; $\chi N = 11.14$ with $f = 0.452$ and 0.548. We could not calculate the boundaries of the G phases into the strong-segregation limit because so many basis functions are required in order to obtain their free energy with accuracy. (We calculate the free energy to a part in 10^4 using up to 60 basis functions.) Noting that their stability regions appear to approach a constant width as χN increases to 20, we extrapolated their phase boundaries in Fig. 1 to $\chi N = 40$ such that the phases remain of constant width and cover the L-H transitions which we could calculate. At $f = 0.37$, this new gyroid phase is stable for $\chi N = 14.9$ to 20.4 which agrees well with measurements for a PS/PI diblock [10] which find the region to extend approximately from χN of 16 to 20. Near the G-L transition, the ratio of the characteristic length of the G phase to that of the L was measured to be 500 Å/210 Å= 2.4 which agrees with our value of 2.45.

In addition to the G phase, we find several other phases which compete for stability along the metastable L-H transition at intermediate segregation. For $f = 0.37$ and $\chi N = 18.496$ where both the L and H have free energies of $F/nk_BT = 3.7926$, the G, monocontinuous CL, and OBDD phases have energies of 3.7856, 3.7898, and 3.8040, respectively. We find two monocontinuous catenoid-lamellar phases nearly degenerate in their free energies. In both phases, the tubes which connect the majority-component lamellae are arranged triangularly, and stagger between adjacent layers. One phase has an *abab...* stacking and the other an *abcabc....* Examining them at weaker segregation, we find the former CL_{ab} to be slightly favored. No solution is found for a CL_a phase with aligned holes. In both staggered phases, the layer spacing is very close to that of the L phase, and both phases have nearly identical hole spacings. The ratio of the hole spacing to the lamellar spacing varies between 1.32 and 1.36 in the region where we find them to be nearly stable. While this is somewhat larger than the two measurements that we are aware of for diblocks, 1.02 [2] and 1.1 [4], it is smaller than the value, 1.49, measured

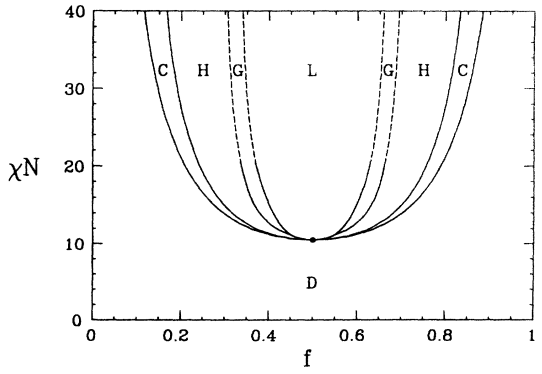

FIG. 1. Phase diagram showing regions of stability for the disordered (D), lamellar (L), gyroid (G), hexagonal (H), and cubic (C) phases. All transitions are first order except for the critical point which is marked by a dot. Dashed lines are extrapolated phase boundaries.

for a diblock-homopolymer mixture in Ref. [5]. The position in the phase diagram where these phases are nearly stable is also consistent with experimental observations, $f = 0.34$ [2], 0.35 [4,6], and 0.33 [5]. Up to the above value of χN, the OBDD phase did not become stable even with respect to L and H phases. However, a calculation for large χN by Olmsted and Milner [18] shows that the OBDD phase does become stable with respect to the L and H phases, but they did not compare it to the G and CL phases.

In the weak-segregation limit, we find that bicontinuous catenoid-lamellar phases are nearly stable along the L-H transition where f is close to 0.5. At the triple point where the L, H, and G phases each have a free energy of $F/nk_BT = 2.752\,72$, the bicontinuous CL_{abc} and CL_{ab} phases have energies of 2.753 58 and 2.754 08, respectively. We do find a solution for a bicontinuous CL_a phase with aligned holes, but it does not exist at the triple point; when it does exist, its free energy is significantly higher than the two with staggered holes. At the triple point, the ratios of the hole spacing to the lamellar spacing for the CL_{abc} and CL_{ab} phases are 1.225 and 1.168, respectively. These phases are consistent with the one observed by Thomas *et al.* [1] for a PS/PB diblock with $f = 0.46$. It may also be the phase observed by both Almdal *et al.* [6] and Hamley *et al.* [4] for a PEP/PEE diblock, which they have labeled as phase (c). Such a phase is suggested because its bicontinuity would explain the large dynamic elastic modulus. The other phase (b) which they observe has a significantly smaller elastic modulus. They postulate that it is a hexagonally moduated lamellar phase. Because we find such phases to be most unstable, we suspect that they observed instead the monocontinuous CL phase which we find very close to being stable.

Our calculation ignores fluctuations. Their effects, while small in general [14,19], can be important close to the transition from the disordered phase [20], and might result in direct transitions from the disordered to the G phase. Further, in light of our results that CL phases are close to being stable, it would be useful to assess whether they can be stabilized either by fluctuations, or by small sheer stresses, such as those applied in Refs. [4] and [6].

We acknowledge useful conversations with A.-C. Shi, F. S. Bates, E. L. Thomas, and S. Milner. This work was supported in part by the NSF under Grant No. DMR 9220733 and NSERC of Canada.

[1] E. L. Thomas *et al.*, Nature (London) **334**, 598 (1988).
[2] R. J. Spontak, S. D. Smith, and A. Ashraf, Macromolecules **26**, 956 (1993).
[3] D. B. Alward *et al.*, Macromolecules **19**, 215 (1986); E. L. Thomas *et al.*, *ibid.* **19**, 2197 (1986); H. Hasegawa *et al.*, *ibid.* **20**, 1651 (1987); T. Hashimoto *et al.*, *ibid.* **26**, 2895 (1993); K. I. Winey, E. L. Thomas, and L. J. Fetters, *ibid.* **25**, 422 (1992).
[4] I. W. Hamley *et al.*, Macromolecules **26**, 5959 (1993).
[5] M. M. Disko *et al.*, Macromolecules **26**, 2983 (1993).
[6] K. Almdal *et al.*, Macromolecules **26**, 1743 (1993).
[7] T. Hashimoto *et al.*, Macromolecules **25**, 1433 (1992).
[8] M. Olvera de la Cruz, Phys. Rev. Lett. **67**, 85 (1991); M. Olvera de la Cruz, A. M. Mayes, and B. W. Swift, Macromolecules **25**, 944 (1992).
[9] G. H. Fredrickson, Macromolecules **24**, 3456 (1991).
[10] D. A. Hajduk *et al.* (to be published).
[11] V. Luzzati *et al.*, Nature (London) **220**, 485 (1968).
[12] K. M. Hong and J. Noolandi, Macromolecules **14**, 727 (1981).
[13] E. Helfand, J. Chem. Phys. **62**, 999 (1975).
[14] G. H. Fredrickson and E. Helfand, J. Chem. Phys. **87**, 697 (1987).
[15] L. Leibler, Macromolecules **13**, 1602 (1980).
[16] J. D. Vavasour and M. D. Whitmore, Macromolecules **25**, 5477 (1992).
[17] The unnormalized basis functions can be found in *International Tables for X-Ray Crystallography*, edited by N. F. M. Henry and K. Lonsdale (Kynoch, Birmingham 1969). Those of the OBDD and G phases appear on pp. 515 and 524–5, respectively.
[18] P. D. Olmsted and S. T. Milner, Phys. Rev. Lett. **72**, 936 (1994).
[19] M. Muthukumar, Macromolecules **26**, 5259 (1993).
[20] S. A. Brazovskii, Sov. Phys. JETP **41**, 85 (1975).